

## **CHAPTER-4**

### **Carbon export and Aeolian flux in the western Arabian Sea**

Global climate has varied in the past at different magnitude. The solar insolation is the major external force which primarily controls the global climate. The solar insolation varies in cyclic pattern associated with the changes in eccentricity, tilt and precession (ETP) called Milankovitch cycles. The eccentricity cycle varies in 100 ka, influencing the very long term changes in the climate. Tilt has a 41 ka cycles of variation while the precession change occurs at 23 ka cycles (Berger, 1988). These changes are the major drivers of global climate through their maxima and minima in heat input to the earth atmosphere. Heat influx varies by the latitude, high flux at equator and low at poles. Atmospheric and ocean circulation work together in levelling the heat difference between latitudes. The internal forces are the heat flux from earth interior, ice volume and greenhouse gas concentration in the atmosphere. The heat flux from the earth interior is well related with the plate tectonics and influence the climate very gradually in the time span of millions of years. Greenhouse gases especially the atmospheric concentration of CO<sub>2</sub> has been identified as the major internal factor which influence the global climate (Frakes et al., 1992). CEF is a major sink for atmospheric carbon dioxide thus it influences global climate (Falkowski et al., 1998). The CEF is much larger than carbon burial since a minor portion of it is ultimately buried in the sediment (Paytan and Griffith, 2007). Increase in CEF has been suggested as a reason for the

reduction in atmospheric CO<sub>2</sub> during Last Glacial Maximum (Martin, 1990). In addition to that the aeolian flux was assumed as the nutrient supplier for the increased CEF during LGM. Though the relation between CEF and aeolian flux were much studied in high nutrient and low chlorophyll (HNLC) regions (Martin, 1990), their relation in other oceanic regions remains less explored. Thus this chapter deals with the reconstruction of CEF and aeolian flux in western Arabian Sea during the last 18.5 ka B.P.

#### **4.1 Estimation of carbon export flux**

Carbon Export Flux (CEF) in the study area is calculated using the method of Francois et al. (1995) from biogenic barium/excess barium (Ba<sub>ex</sub>) flux measured in the 4018 sediment core. There are few prerequisites to be met before the use of Ba<sub>ex</sub> flux, which are, (1) understanding of Ba sources in study area, (2) Ti sources, (3) Ba/Ti ratio in source material, (4) modern relationship between Ba<sub>ex</sub> flux and export flux.

Ba in marine sediments may have been derived from various sources, (1) detrital, (2) scavenging of dissolved Ba by Mn hydroxides, (3) Barite crystals formed during organic matter degradation (Paytan and Griffith, 2007). The calculation of Ba<sub>ex</sub> itself removes the detrital derived contribution of Ba. Scavenging of Ba by Mn hydroxides can act as major removal mechanism where the availability of Mn is in excess. By studying Ba<sub>ex</sub> flux to sediment traps in the Arabian sea, Nair et al. (2005) have reported that the scavenging of Ba by Mn hydroxides occurs when the Mn<sub>ex</sub> is more than 200 ppm (Figure 4.1). This is not the case in 4018 record, the Mn<sub>ex</sub> remains below 200 ppm through out the record. No significant relationship found between Ba<sub>ex</sub> and Mn<sub>ex</sub> during last 18.5 ka also denies the presence of scavenged Ba (Figure 4.1). An increase in Ba/Corg along with depth in western Arabian Sea (Nair et al., 2005) suggest that the organic carbon remineralization is the main source for Ba<sub>ex</sub>. The Al and Ti content in marine sediment are used as proxies for the lithogenic fraction (Murray and Leinen, 1996). However the use of Ti normalization in marine settings away from volcanic sources has been suggested to eliminate the problems associated with Al (Paytan and Griffith, 2007). Increasing evidence for the non-terrigenous component of Al in marine sediments like Al association with diatom tests or Al adsorbed onto sinking particles complicates the use of Al in Ba<sub>ex</sub> estimation (van Bennekom et al., 1989; Murray et al., 1993; Murray and Leinen, 1996; Dixit et al., 2001). The estimation of Ba<sub>ex</sub> in marginal marine settings is more complex than the open ocean where the detrital input is low. The precise value of Ba/Ti ratio in the detrital material is very difficult to measure as it can be a mixture of

different provenance. The detrital content in the present study area is predominately derived from the surrounding deserts through aeolian flux. Mostly the Ba/Ti ratio of PAAS (Post Archean Australian Shale) or UCC (Upper Continental Crust) is used as representative for detrital material (Mclanen, 2001). In the present study the Ba/Ti of UCC is used to represent the detrital component.

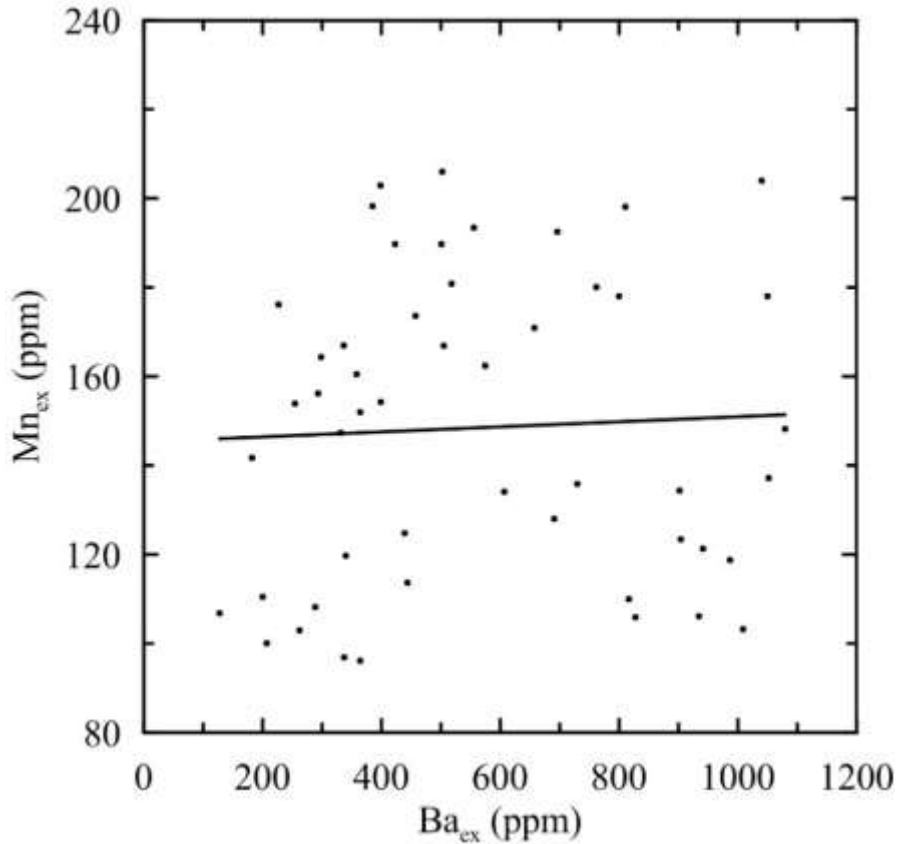


**Figure 4.1:** Comparison of Ba excess with Mn excess in the 4018 sediment core record.

Apart from the above mentioned issues, the preservation efficiency of Ba in sediment may affect the carbon export flux estimation. Preservation efficiency is calculated by measuring the difference between Ba flux in sediment trap and surface sediment. Nair et al. (2005) observed ~58% of the Ba in the settling particles is preserved in surface sediments of the western Arabian Sea. So the equation given below is used to get preservation corrected Ba<sub>ex</sub> (P.Ba<sub>ex</sub>) flux,

$$P. Ba_{ex} flux = Ba_{ex} flux / 0.58$$

Finally export flux have been computed using Francois et al. (1995) equation,

$$CEF = 1.98 * (P. Ba_{ex} flux)^{1.41}$$

Where the CEF in gC/m<sup>2</sup>/y and preservation corrected Ba<sub>ex</sub> flux in ug/cm<sup>2</sup>/y.

## 4.2 Aeolian flux

There is no specific measurement for aeolian flux in marine sediments (Kohfeld and Harrison, 2001). Non-carbonate content of open marine sediment is widely accepted as aeolian fraction except for the regions with high siliceous productivity or ice-rafted debris flux (Kohfeld and Harrison, 2001). The biogenic silica content in 4018 core varies significantly (Balaji et al., 2018), therefore it has been considered for the estimation of aeolian flux in the present study. The weight percent of aeolian content is determined by isolating the terrigenous fraction of the sediment by eliminating carbonate, opal and organic matter (Rea, 1994; Kohfeld and Harrison, 2001). There is no fluvial influx to the study area due to the arid climate (Sirocko et al., 2000) in the surrounding regions, so the non-biogenic fraction is considered as aeolian in this study.

$$\text{Aeolian fraction (AF)} = 1 - \text{CaCO}_3 - \text{Organic carbon} - \text{Biogenic silica}$$

The concentration of  $\text{CaCO}_3$ , organic carbon and biogenic silica for 4018 sediment core were adopted from Tiwari et al. (2010) and Balaji et al. (2018). Other authigenic contents ( $\text{Ba}_{\text{ex}}$ ,  $\text{Mn}_{\text{ex}}$ ) were not considered due to their low concentration (<0.1%).

## 4.3 Results

### 4.3.1 $\text{Ba}_{\text{ex}}$ Concentration

Down core variation of  $\text{Ba}_{\text{ex}}$  concentration (now on  $\text{Ba}_e\text{C}$ ) and its percentage in total Ba is shown in figure 4.2. The concentration minima is observed at 15.5 ka B.P. and the maxima at the surface of sediment core (modern). Overall it shows an increasing trend with lows and highs at different time slices. At the bottom of the core i.e. at 18.5 ka B.P. the  $\text{Ba}_e\text{C}$  was 200 ppm, then it increased to 450 ppm in next 2 ka (18.5-17 ka B.P.). After 17 ka B.P., the concentration is seen to decrease attaining the lowest value of 127 ppm at 15.5 ka B.P. From 15.5 ka B.P., the concentration of  $\text{Ba}_e\text{C}$  increased to 550 ppm at 13 ka B.P. Abrupt decrease in  $\text{Ba}_e\text{C}$  (550 to 220 ppm) is observed after 13 ka B.P. In the following one ka i.e. from 13 to 12 ka B.P.,  $\text{Ba}_e\text{C}$  slightly decreases (220 to 200 ppm). Four fold increase in  $\text{Ba}_e\text{C}$  (200 to 800 ppm) is observed between 12 to 10 ka B.P. However, 10 ka B.P. onwards, the value of  $\text{Ba}_e\text{C}$  again decreases with two lows (~400ppm) in first one thousand years and reaches 570 ppm at 8 ka B.P. After 8 ka B.P.  $\text{Ba}_e\text{C}$  shows an increasing trend until it attains 1050 ppm at 6 ka B.P. In the last 6 ka,  $\text{Ba}_e\text{C}$  shows a constant high value (>1000 ppm) with three lows centred at 3.7, 2.7 and 0.5 ka B.P. Ba excess percentage in total Ba

varies between values from 36 to 91. It follows the variation trend of  $Ba_{eC}$  until 10 ka B.P., remains more or less constant at ~85 % subsequently. An abrupt shift at 13 ka B.P. is observed in this parameter also (84 to 65 %).

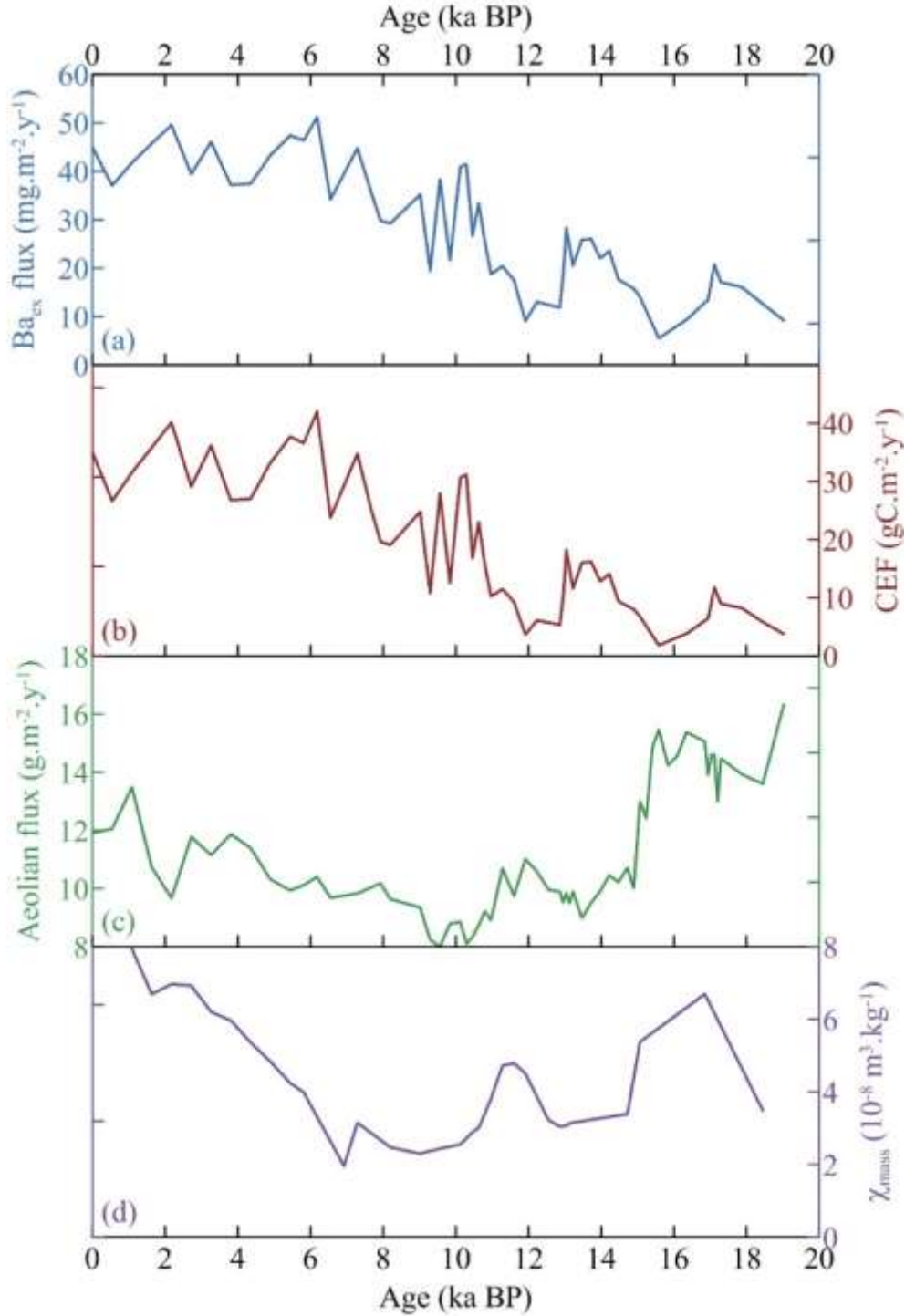


**Figure 4.2:** Temporal variation of productivity and Aeolian flux in 4018 sediment core.

### **4.3.2 Carbon export flux**

Export flux in north western Arabian Sea shows 20 fold variation in last 18.5 ka (Figure 4.2). Lower values observed at the bottom of the sediment core. It was 4 gC/m<sup>2</sup>/y at 18.5 ka B.P., then increased around three times gradually and reached 12 gC/m<sup>2</sup>/y at 17 ka B.P. After 17 ka B.P. it gradually decreased in next 1.5 ka and attained its minimum of 2 gC/m<sup>2</sup>/y at 15.5 ka B.P. After attained its minimum value, export flux again gradually increased from 2 to 19 gC/m<sup>2</sup>/y until 13 ka B.P. with a low value (12 gC/m<sup>2</sup>/y) centred at 12 ka B.P. There is an abrupt negative shift in export flux observed at 13 ka B.P. as same as Ba<sub>c</sub>C. Again there is a decrease observed between 13 to 12 ka B.P. from 6 to 4 gC/m<sup>2</sup>/y. After 12 ka B.P. export flux sharply increases to 32 gC/m<sup>2</sup>/y in 2 ka and then it decreases to 19 gC/m<sup>2</sup>/y in another 2 ka with two lows between 9 to 10 ka B.P. From 8 ka B.P. onwards export flux raises until 6 ka B.P. (42 gC/m<sup>2</sup>/y) and then it falls down to 27 gC/m<sup>2</sup>/y at 3.7 ka B.P. In the next 1.5 ka export flux shows positive shift from 27 to 40 gC/m<sup>2</sup>/y. After 2.2 ka B.P. export flux slightly decreased and reached the modern value of 35 gC/m<sup>2</sup>/y. Overall export flux shows an increasing trend in the last 18.5 ka in the study area.

### **4.3.3 Aeolian flux**

Dust concentration ranges from 15 to 35 % during last 18.5 ka B.P. in the study area (Figure 4.2). Highest concentration (~35 %) is observed at the bottom and then it decreased to 30 % at 18 ka B.P. After 18 ka B.P., dust concentration again increased and peaked at 15.5 ka B.P. There is an abrupt negative shift in dust concentration (35 to 22 %) observed after 15.5 ka B.P. for about 0.5 ka. Subsequently, it decreased to its lowest value at 9.5 ka B.P. except positive shifts at 12 to 11 ka B.P. After 9.5 ka B.P., the dust concentration continuously increased until 3 ka B.P. with minor variations. During the last 3 ka B.P., there was a minima observed at 2.5 ka B.P. and a maxima at 1 ka B.P. Dust flux also resembles trend of dust concentration throughout the studied timespan. It varied between 8 to 16 g.m<sup>-2</sup>.y<sup>-1</sup> with lowest value being observed at 9.5 ka B.P. and maximum at 15.5 ka B.P.

## **4.4 Discussion**

### **4.4.1 Palaeoproductivity in the study area during the last 18.5 ka B.P.**

The CEF indicates significant variation in productivity in the western Arabian Sea during the last 18.5 ka B.P. The lower CEF values during 18.5 to 16 ka B.P., indicate low surface productivity coinciding with the Last Glacial Maximum (LGM). High surface productivity in the

western Arabian Sea occurs during the summer months due to southwest monsoon induced upwelling (Haake et al., 1993). The weak upwelling might be the cause for the observed low CEF in the present record. The carbon burial efficiency shows high values during this time span (Figure 4.3). The carbon burial efficiency is estimated as a percentage of organic carbon preserved in the sediment (organic carbon flux) out of CEF. The increased carbon burial efficiency indicates stratified oceanic condition which would reduce the remineralisation of CEF (Lee, 1992). Overall LGM is marked by low surface productivity and increased burial of organic carbon in the western Arabian Sea in agreement with the previous studies that observed low productivity during LGM in the north western part of the basin (Sirocko et al., 2000; Ivanochko et al., 2005). The low productivity in the study area during LGM, as compared to modern, suggests its insignificant role in the biological pump for the reduction of CO<sub>2</sub> during LGM.

From 16 to 13 ka B.P. the CEF display relatively high values as compared to LGM. However the reduced carbon burial efficiency observed during this time gap indicate increased remineralisation caused by vertical mixing of water column/upwelling. Balaji et al. (2018) noted a coeval enhanced southwest monsoon phase based on the biogenic silica flux. Isaji et al. (2015) indicated an accelerated southwest monsoon in the western Arabian Sea during interglacial based on Zr/Hf ratio from sediment cores retrieved from Gulf of Aden. Anand et al. (2008) and Saher et al. (2007) have observed low sea surface temperature during 16 to 13 ka B.P. and attributed to increase in southwest monsoon induced upwelling. Overall the time gap between 16 to 13 ka B.P. is characterised by the high productivity and increased vertical mixing in the western Arabian Sea. Reduced CEF, similar to LGM, is observed between 13 to ~11.7 ka B.P. indicating low surface productivity. However the carbon burial efficiency show higher values during this time period. The CEF along with carbon burial efficiency suggests low productivity with increased burial which in turn suggests stratified oceanic conditions (Figure 4.3). Reduced strength of upwelling observed in the western Arabian Sea (Balaji et al., 2018) might have caused the reduction in CEF during 13 to 11.7 ka B.P. The CEF has increased more than six times from 5 gC.m<sup>-2</sup>.y<sup>-1</sup> at 11.7 ka B.P. to 30 gC.m<sup>-2</sup>.y<sup>-1</sup> at 10 ka B.P., at the beginning of Holocene. However a simultaneous reduction in carbon burial efficiency point to increased oxygen content or remineralisation in the water column. This altogether suggest high nutrient conditions in the western Arabian sea caused by strengthening of upwelling. From 10 to 8 ka B.P. the CEF has decreased gradually but the low CEF observed at 8 ka B.P. is much higher than LGM and 13-11.7 ka B.P. While carbon burial

efficiency remains constant during 10 to 8 ka B.P. suggests minor changes in the environment. After 8 ka B.P. the CEF has increased to the levels observed at 10 ka B.P., indicate high surface productivity. In the last 8 ka CEF has sustained above  $30 \text{ gC.m}^{-2}.\text{y}^{-1}$  with millennial scale oscillations. The CBE shows minor decrease after 8 ka B.P. and remained below 2% till present. Therefore the last 8 ka B.P. has been interpreted as high productive period with strengthened upwelling and vertical mixing.

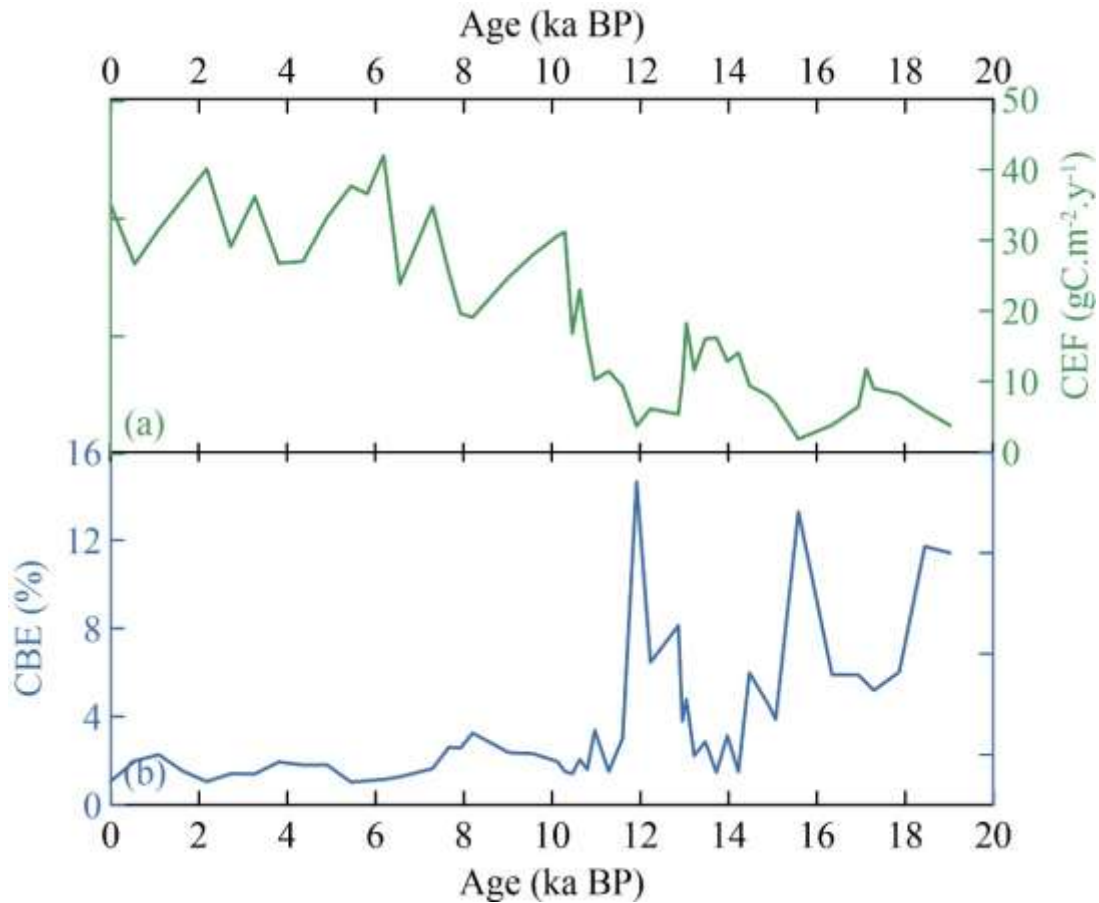


**Figure 4.3:** Temporal changes in the Carbon export flux (CEF) and Carbon burial efficiency (CBE) in the 4018 sediment core.

#### 4.4.2 Aeolian flux in the western Arabian sea

Aeolian flux in the marine sediments is a good recorder of climate over the adjacent land mass and atmospheric pattern. In the modern condition, Arabian Sea receives the third largest supply of aeolian content in the world. Pattern of aeolian flux to the western Arabian Sea during the last 18.5 ka B.P. has been reconstructed. In addition to the aeolian flux the magnetic susceptibility record of 4018 sediment core also discussed. The positive correlation observed

between aeolian flux and magnetic susceptibility in the present sediment record validates the use of magnetic susceptibility as a proxy for terrigenous flux in marine systems (Figure 4.4).

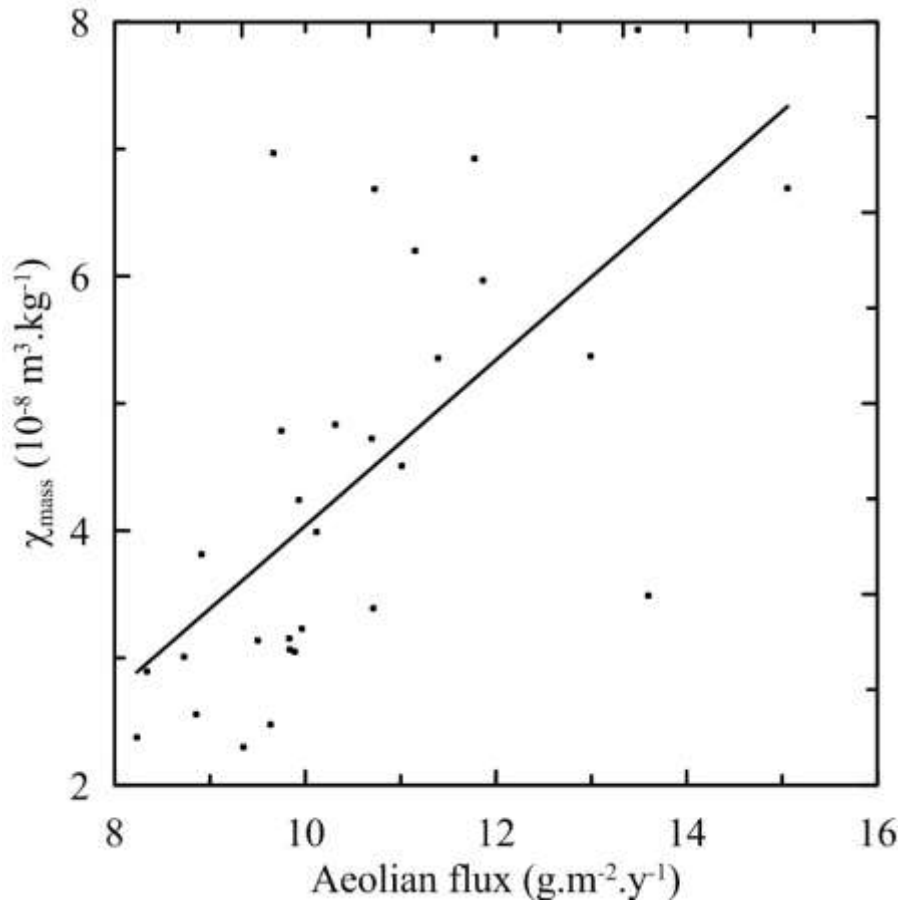


**Figure 4.4:** Aeolian flux versus magnetic susceptibility in 4018 sediment core. The linear relation between them suggests aeolian flux is the major source of magnetic mineral for the present sediment core.

Aeolian flux to the western Arabian Sea show multi-millennial scale variations during the last 18.5 ka B.P. (Figure 4.5). High aeolian flux were observed during 18.5 to 15 ka B.P. suggest dry and arid climate conditions in the surrounding landmass. The source of this high aeolian flux can be delineated using the Mg content in the sediment core record. Sirocko et al. (1993) has suggested the use of Mg content in marine sediment of North western Arabian Sea as a proxy for Arabian dust. In the present record the Mg concentration shows maximum value at around 16 ka B.P. indicating the aeolian flux from Arabian landmass. This interpretation is supported by the previous study by Clark and Fontes, (1990) based on carbonates from hyper-alkaline groundwater in Oman, where they noted an arid climate around 19 ka B.P.

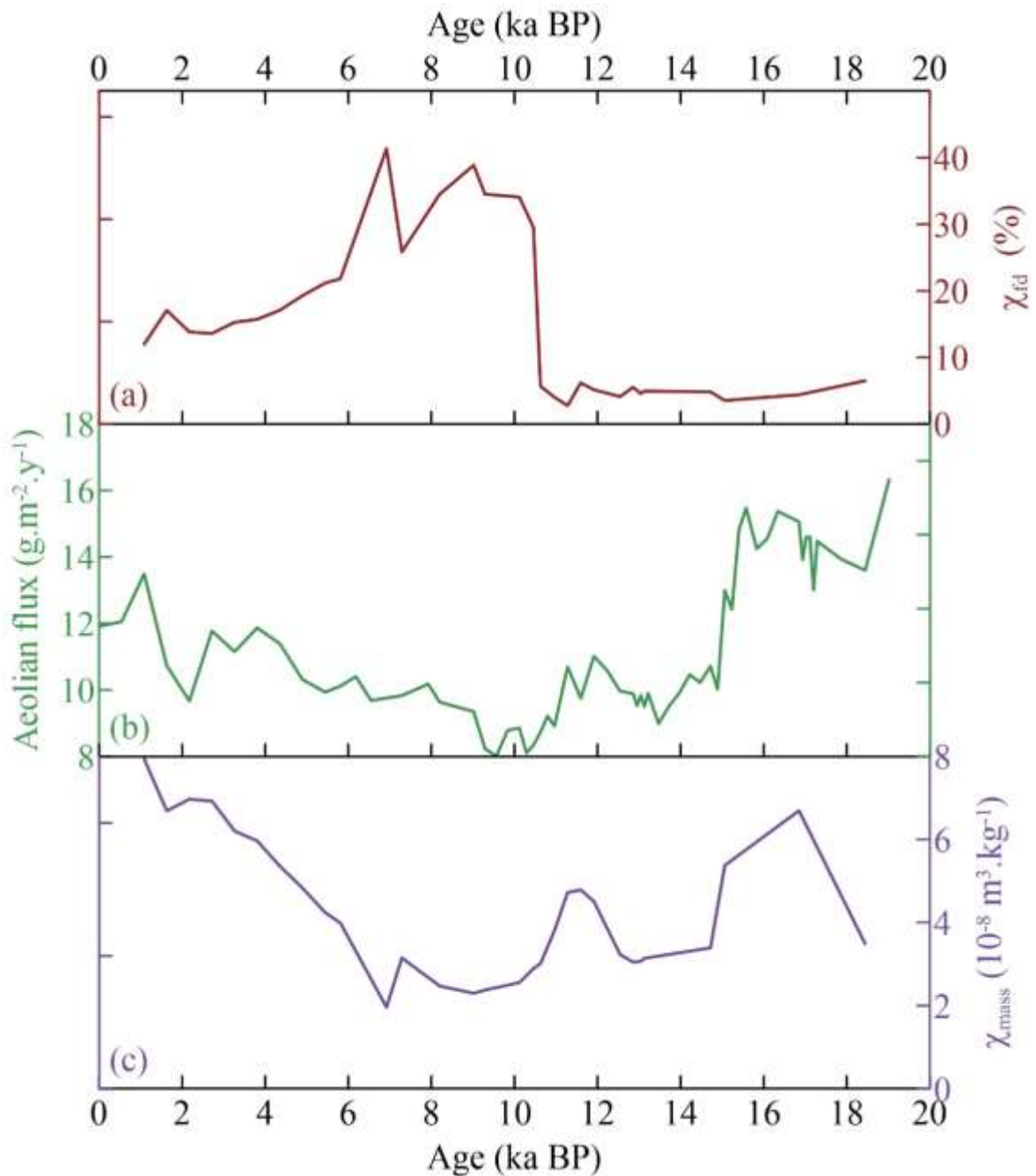


**Figure 4.5:** Aeolian flux and magnetic susceptibility record of 4018 sediment core for the last 18.5 ka B.P.

The magnetic susceptibility also shows high values around 16 ka B.P. suggesting increased supply of magnetic minerals to the western Arabian Sea from the nearby continents. Further there is an abrupt reduction in aeolian flux of about 30% has been noted at 15 ka B.P. This abrupt reduction has occurred within a century or two and marks a major change in the climate of the adjacent land mass. Fleitmann et al. (2007) has noted wetter climate condition at 15 ka B.P. in the

Arabian landmass. Tierney and deMenocal (2013) has observed humid conditions in the east African climate at the same time. Sirocko et al. (2000) and Isaji et al. (2015) also observed a change in the provenance of terrestrial material at around 15 ka B.P. They had shown that the lithogenic content in the western Arabian Sea sediments are mainly derived from Horn of Africa region at 15 ka B.P. This indicates the intensification of southwest monsoon, the influence of southwest monsoonal winds in the study area might have reduced the aeolian supply from Arabian Peninsula. Further the wetter conditions in the Horn of Africa region at 15 ka B.P. might have had a negative impact on aeolian supply. The reduced magnetic susceptibility observed during 15 to 13 ka B.P. marks reduction in magnetic mineral content that in turn point to variation in the source. After 13 ka B.P., there was a marginal increase in aeolian flux observed in the present sediment core record pointing towards arid conditions. Magnetic susceptibility also show a positive peak between 13 to 11 ka B.P. However, the Mg concentration shows insignificant change during 13 to 11 ka B.P. that refutes the possible influence of north easterlies and Arabian dust. Therefore the observed changes in aeolian flux at this time might have been caused by the change in climate over the source region alone, without change in provenance. Hence it has been suggested that the climate in the Horn of Africa region during 13 to 11 ka B.P. was arid. This interpretation is in agreement with previous study by Tierney and deMenocal (2013) on leaf wax data from Gulf of Aden where they observed an arid climate conditions during 13 to 11 ka B.P. The lowest aeolian flux were observed after 11 ka B.P., particularly around 10 ka B.P., in the present sediment core suggests wetter conditions in the source region.

Since 10 ka B.P. the aeolian flux to the western Arabian Sea has increased which is also observed in magnetic susceptibility. While the Mg concentration did not show any significant change during the last 10 ka B.P., indicating similar conditions i.e. less aeolian supply from Arabian landmass. As per the modern conditions the maximum aeolian flux is derived from Horn of Africa region to the western Arabian Sea during southwest monsoon season. There is less transport from north eastern part, Arabian Peninsula, to the western Arabian Sea during the northeast monsoon season. The invariant Mg content dismiss the influence of northeast monsoon and the productivity records show strengthened southwest monsoon during the last 10 ka B.P. However the Horn of Africa remained the source region there is an increase in the magnetic mineral content and aeolian flux. This indicates change in the climatic conditions at the Horn of Africa region. The increased aeolian flux can be attributed to increased wind over the Horn of

Africa region due to intensified southwest monsoon. However the frequency dependent magnetic susceptibility ( $\chi_{fd}$ ) depicts an abrupt increase around 11 ka B.P. indicating the increase of fine-grained magnetic mineral supply (Figure 4.5). Maher and Thompson (1995) noted increased production of fine-grained magnetic mineral with increased wet/dry cycles in regions of high rainfall. Tierney and deMenocal (2013) observed wetter conditions in Northeast Africa at the beginning of Holocene caused by African humid period (AHP). Balaji et al. (2018) observed increased southwest monsoon inferred at the beginning of Holocene. Increased wetter conditions in the northeast African region lead to more production of fine-grained magnetic mineral, which is carried and deposited to the study area by the strengthened southwest monsoonal winds. This interpretation is supported by the late Holocene reduction in  $\chi_{fd}$  (Figure 4.5) along with gradual decline of AHP (Tierney and deMenocol, 2013). The aeolian flux and magnetic susceptibility gradually increased throughout Holocene and the productivity records show an increased southwest monsoonal upwelling. Therefore the higher aeolian flux is attributed to the increased aridity in east Africa region along with strengthened southwest monsoonal winds that caused more aeolian flux.

#### **4.4.3 Influence of Aeolian flux on productivity**

Aeolian flux has been identified as an important source for nutrients to the oceanic surface productivity especially for the remote oceanic regions with abundant macro-nutrients (Martin, 1990). Because the aeolian flux act as a supplier of micronutrients like Fe which is important for the phytoplankton growth. Though the present study area is not considered as a high nutrient region like southern ocean, but recent studies have revealed that the western Arabian Sea mimics High Nutrient Low Chlorophyll (HNLC) conditions during the peak monsoon season (Naqvi et al., 2010). Liao et al. (2016) observed strong coupling between atmospheric deposition and primary production in western Arabian sea upwelling region. Banerjee and Kumar (2014) noted episodic increase of primary production in central Arabian Sea mainly driven by atmospheric deposition of iron and other nutrients. Therefore the aeolian flux and carbon export flux were compared in the present study to give a preliminary assessment on the long term relation between them. The scatter plot of CEF versus aeolian flux for the last 18.5 ka B.P. from 4018 sediment core record shows a negative correlation between them (Figure 4.6). However the separate plots for particular time gaps show varying relation between CEF and aeolian flux.

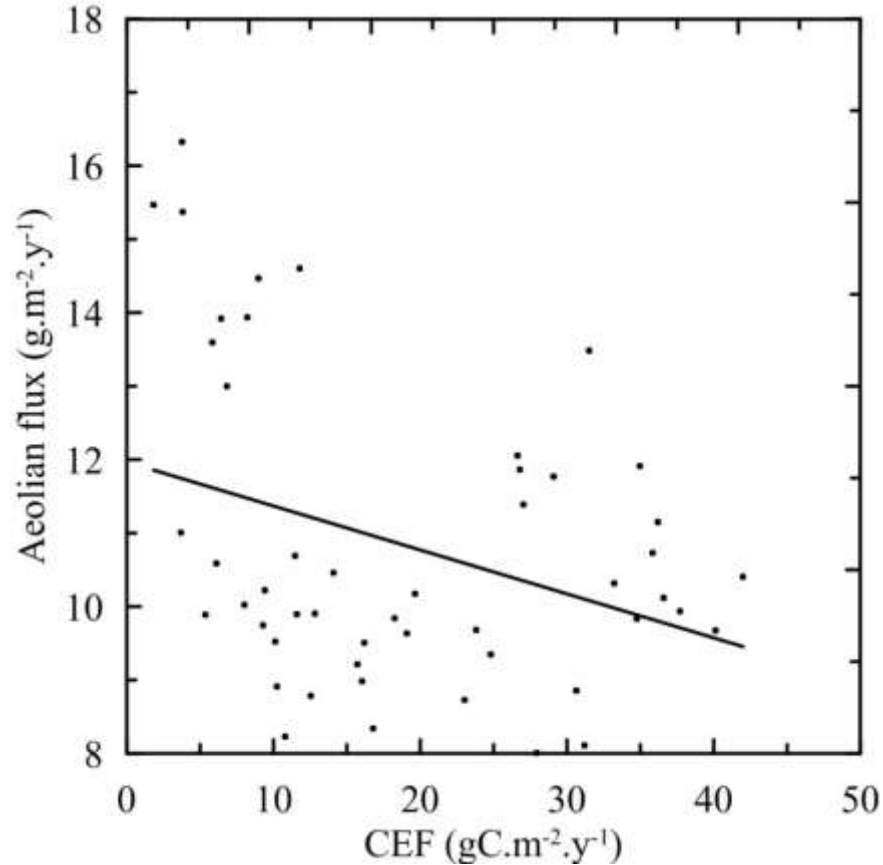


**Figure 4.6:** Aeolian flux versus Carbon export flux in the present sediment core record for the last 18.5 ka B.P.

The scatter plot of aeolian flux versus CEF for the duration from 18.5 to 11.7 ka B.P. (Figure 4.7) shows a negative correlation, which suggests that the increase in aeolian flux leads to decrease in the surface productivity. This is in contradiction to the conventional idea that the increase in aeolian flux would increase the micro-nutrient (Iron, Zinc, etc) availability that leads to higher productivity (Martin, 1990). However the positive correlation between aeolian flux and productivity is valid in the presence of macronutrients (like Nitrogen, Phosphorous, etc). If there is not enough macronutrients then the aeolian flux may not have any influence on the productivity but it can reduce sun light penetration through turbidity. Thus it is inferred that the availability of macro-nutrients were limited in the western Arabian Sea during 18.5 to 11.7 ka B.P. Though the productivity reconstruction suggests the southwest monsoon induced upwelling was high during 15 to 12.9 ka B.P. (Balaji et al., 2018), the CEF to aeolian flux relation remained negative which indicates that the upwelling was not enough to keep the surface waters with macro-nutrients in excess.

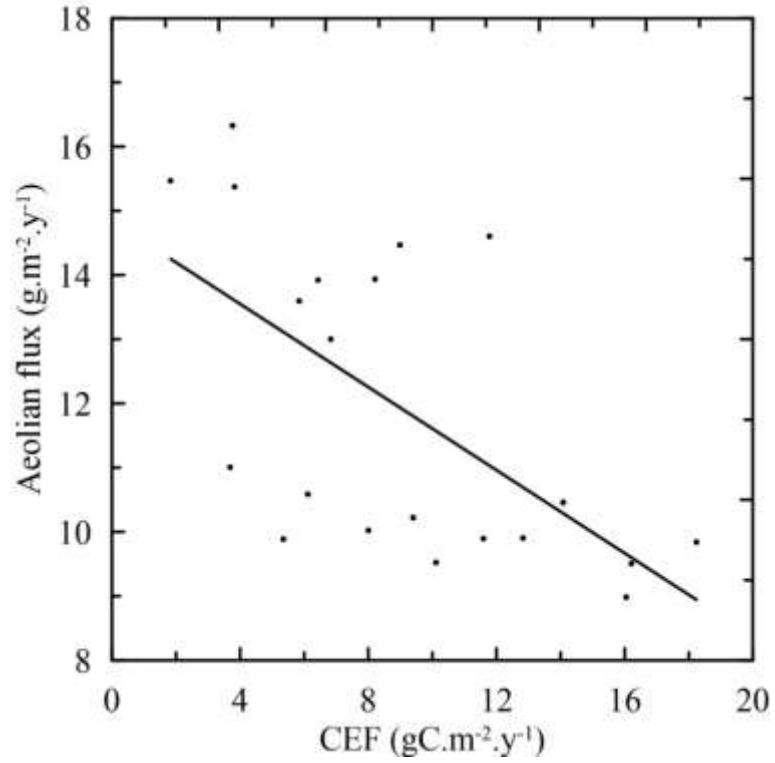


**Figure 4.7:** Aeolian flux versus CEF in the 4018 sediment core record for the time gap from 18.5 to 11.7 ka B.P.

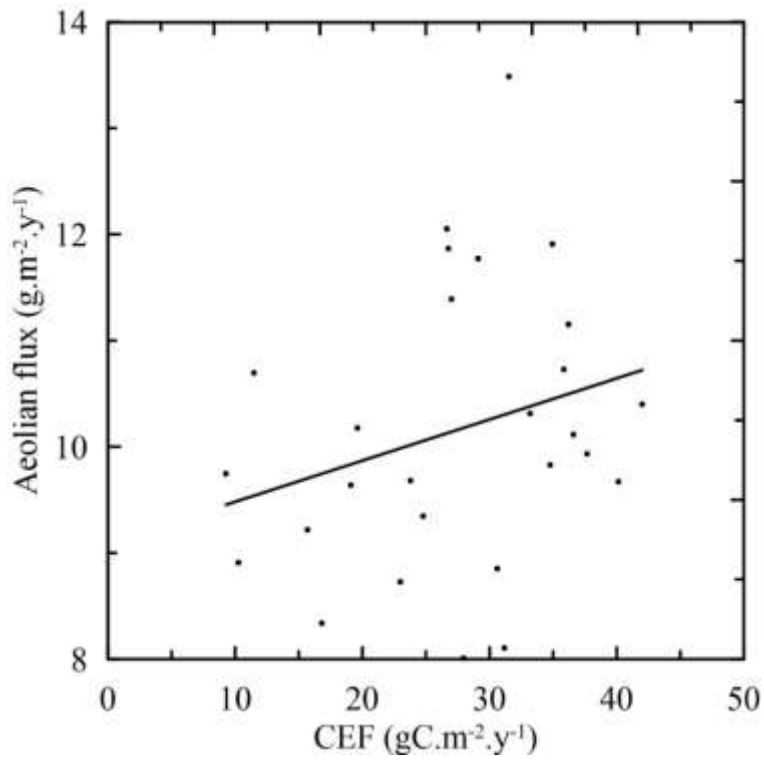


**Figure 4.8:** Aeolian flux versus CEF in the present record during Holocene (last 11.7 ka B.P.).

The aeolian flux and CEF shows positive correlation during the last 11.7 ka (Figure 4.8). Based on productivity, it is inferred that the southwest monsoon induced upwelling was high throughout Holocene and caused high productivity. The increased upwelling might have created HNLC like conditions in the study area during Holocene. The increased aeolian flux could have supplied more micro-nutrients and lead to increased CEF throughout Holocene. Therefore the present study infers that the HNLC like condition during southwest monsoon in Arabian Sea set in at the beginning of Holocene. It is also indicated that the northern Arabian Sea in general and north-western in particular are not the parts of the last glacial biological pump that reduced atmospheric CO<sub>2</sub> to LGM levels.